The theory of metal - ceramic interfaces

1996 J. Phys.: Condens. Matter 8 5811

(http://iopscience.iop.org/0953-8984/8/32/003)

J. Phys.: Condens. Matter **8** (1996) 5811–5836. Printed in the UK

TOPICAL REVIEW

The theory of metal–ceramic interfaces

M W Finnis

Atomistic Simulation Group, School of Mathematics and Physics, Queen's University of Belfast, Belfast BT7 1NN, UK

Received 10 April 1996

Abstract. The theory of metal–ceramic interfaces is a collection of approaches which are complementary. They range from thermodynamic modelling based on empirical correlations, through the image model of adhesion, semi-empirical tight-binding calculations, to first-principles calculations based on applying the density functional theory or Hartree–Fock theory. This article reviews the present state of theoretical calculations, with particular reference to electronic structure and adhesion. A section on the thermodynamic background clarifies the concept of work of adhesion which is the goal of many calculations. Cluster models and periodic slabs have been considered, both self-consistent and non-self-consistent. The most sophisticated and complete calculations have been made for metals on MgO and alumina. There a consistent picture of the nature of the bonding has emerged, although there are still significant unexplained discrepancies in numerical values.

1. Introduction

To understand and control metal–ceramic interfaces is an important goal for an extraordinary variety of industrial and scientific reasons, as can be appreciated by glancing through the current journals relating to materials science and technology. Coatings of oxide which function as thermal barriers or as a natural corrosion protection are of concern to the manufacturers of jet engines and equipment for power generation, who seek to improve lifetimes and efficiency. The technology of brazing relies on the efficient wetting of ceramic by metal. Light bulbs rely on metal–ceramic seals. Fibre–matrix composites owe their mechanical properties to the metal–ceramic interfaces they contain. In the chemical industry, catalyst support and sensor technology depend on the properties of metal–ceramic interfaces. The electronics industry depends on the properties of such interfaces for packaging and in components such as rectifiers and MOSFETs. In particular the recording industry is concerned with their atomic-scale properties in the design of magnetic recording heads and in advanced electronic and optical devices involving thin films or multilayers. Medical implants, for example in dentistry, depend on the adherence and integrity of metal–ceramic bonds.

The incentive to provide a theoretical understanding of metal–ceramic adhesion has increased as more refined experimental probes are becoming available to explore the atomic and electronic structure of interfaces. High-resolution transmission electron microscopy can reveal the atomic structure at interfaces to 0.02 nm accuracy (Mayer *et al* 1990, Ernst *et al* 1991, Merkle 1991, Trampert *et al* 1992, Ikuhara and Pirouz 1993, Gutekunst *et al* 1994) and their chemical structure can be probed to almost atomic resolution by electron energy-loss spectroscopy (Bruley *et al* 1994). Recently atomic-scale studies of segregation

0953-8984/96/325811+26$19.50

at metal–ceramic interfaces have been made by atom probe field-ion microscopy (Jang *et al* 1993, Chan *et al* 1995, Shashkov and Seidman 1995a, b). With the incentive of understanding the conditions of catalysis, the plethora of surface science techniques has also been focused on thin films of metal deposited on oxide surfaces or vice versa (Pan *et al* 1993, Diebold, *et al* 1994, Libuda *et al* 1994a, b, Bertrams *et al* 1995, Diebold *et al* 1995, Freund 1995).

Using the electronic theory of *bulk* materials properties, notably the density functional theory, it has been possible for some time to calculate from first principles the equilibrium crystal structures, cohesive energies, lattice parameters, elastic moduli, and in some cases phase diagrams of crystalline solids (Pettifor and Cottrell 1992). Nevertheless, even in single-phase systems, mechanical properties and strength, depending as they do on defect concentrations and defect dynamics are not yet predictable from basic, atomic-scale theory. The theory of heterogeneous interfaces is in a still more primitive state, but it has begun to catch up with that of bulk materials. The electronic theory of metal–ceramic bonding is not yet able to predict interface mechanical properties for a given pair of materials, but it is starting to predict the primitive quantities on which those properties essentially depend, such as structures and energies. This process has been enabled by the development of theoretical models and by the rapidly increasing performance of computers.

In this article I review the main theoretical approaches which have been taken and the progress which has been made in understanding metal–ceramic cohesion, at both qualitative and quantitative levels. Until recently most progress seems to have been made in rationalizing the data on different metal–ceramic pairs not by direct calculation using first-principles (*ab initio*) models or semi-empirical models of total energy, but by a judicious combination of thermodynamic data and empirical modelling, as described in the reviews by Naidich, Li and Howe (Naidich 1981, Li 1992, Howe 1993). I therefore briefly discuss such approaches in section 3, but emphasize here that there is still very little basic understanding of the empirical correlations which are observed. Besides these reviews, a useful collection of papers and references up to 1991 are the proceedings of the conferences on metal–ceramic interfaces at Santa Barbara (Rühle *et al* 1990) and Irsee (Rühle *et al* 1992). Since previous reviews have covered the experimental data and correlations in detail, the present one focuses on atomistic and electronic theories. Furthermore, since most progress has been made on interfaces with wide-band-gap oxides, most of my detailed examples concern these.

A concept which figures prominently in both atomistic and phenomenological discussions of metal–ceramic adhesion is the *work of adhesion*. In the literature it has at least two different meanings, often without a clear distinction. The following section is intended to clarify the physics of this concept and to define some terminology.

2. Thermodynamic background

An important fundamental quantity which controls the mechanical strength of a metal–ceramic interface is the ideal *work of separation* W_{sep}, the reversible work needed to separate the interface into two free surfaces, a thought experiment whereby plastic and diffusional degrees of freedom are supposed to be suppressed. Other factors are important in any practical attempt to predict the strength of an interface, such as the plastic and elastic properties of the materials, the geometry of the loading, the presence and size of flaws and of residual internal strains. Nevertheless the work of separation has a special status as an interfacial property because it is fundamental to mechanical properties, like a state function it can be defined unambiguously for ideal systems and therefore, at least in principle, it

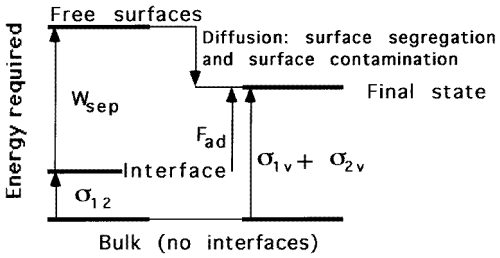

Figure 1. A diagram of the energies involved in cleaving an interface, excluding plastic processes.

can be calculated. The energy needed in a cleavage experiment will always exceed W_{sep}, but, other things being equal, the greater W_{sep}, the greater the energy needed to cleave the interface, so it would be a useful quantity to know. In terms of the surface and interfacial excess free energies of the materials, the ideal work of separation is given by the Dupré equation:

$$W_{sep} = \sigma'_{1v} + \sigma'_{2v} - \sigma_{12} \tag{2.1}$$

where 1 and 2 denote the materials and v the vapour. It is a potentially useful equation, because surface energies can sometimes be obtained from experiment; however, there are pitfalls. As mentioned before, the measured adhesion energy in any conceivable cleavage experiment would exceed the ideal value of the Dupré equation, due to dissipative processes. Less obviously, these dissipative processes, besides the plastic processes involving movement of dislocations which generate heat, include the diffusion processes of chemical equilibration. Such processes are bound to take place in a multicomponent system: the concentration of any segregants at the freshly created surfaces will at first be the same as they were at the interface, but only for an instant. Diffusion will then take place, which will adjust the concentrations to new values appropriate to free surfaces. When these equilibrium values have been reached—which may be long after the plastic dissipation has run its course—the surface energies will have dropped from the instantaneous values they had after the cleavage (denoted by the primed sigmas in equation (2.1)) to their equilibrium values as determined by the bulk compositions of materials 1 and 2 and the composition of the vapour (see figure 1).

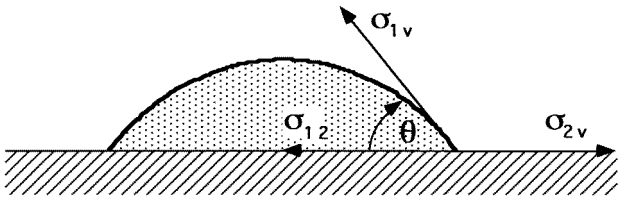

Figure 2. The contact angle θ of a sessile drop.

I have dwelt on this point because it is common to identify the surface energies, primed in the Dupré equation above, with those in the Young equation for the contact angle θ of a

liquid drop of material 1 on a surface of material 2 (see figure 2):

$$\cos\theta = \frac{\sigma_{2v} - \sigma_{12}}{\sigma_{1v}}. \tag{2.2}$$

The smaller the contact angle, the greater the *wettability* of material 2 by material 1. It is appealing to try to connect the work of separation to the contact angle because the latter is directly measurable. The correct procedure, however, as pointed out by Tomsia and co-workers (Tomsia *et al* 1995), is to define a different work of *adhesion*, which is the reversible *free-energy* change for making free surfaces from interfaces, whereby the free surfaces are in equilibrium with the solid and gaseous components:

$$F_{ad} = \sigma_{1v} + \sigma_{2v} - \sigma_{12}. \tag{2.3}$$

Whereas a direct measurement of W_{sep} is hardly possible, the contact angle can be measured, and the interfacial energy can be eliminated between (2.2) and (2.3) to give a measured value of the work of adhesion F_{ad} in (2.3) in terms of one of the surface energies:

$$F_{ad} = \sigma_{1v}(1 + \cos\theta). \tag{2.4}$$

I have followed the physical convention of Tomsia *et al* by calling W_{sep} the work of *separation* and F_{ad} the work of *adhesion*, although Tomsia *et al* used for both the symbol W_{ad}, and distinguished them by the font. The distinction between W_{sep} and F_{ad} is fundamental in all systems having more than one component.

Another obstacle to obtaining the mechanical quantity W_{sep} is that in equation (2.1) both components are solid, whereas equation (2.2) strictly refers to a liquid–solid contact. Quantitative examples of these difficulties are given by Howe (1993).

In the case of metal on oxide we are dealing with at least a two-component system, but usually more. If oxygen can diffuse to the interface, the partial pressure of oxygen in the system will directly affect the value of σ_{12} in (2.1) and (2.2), as well as the values of all the surface energies. W_{sep} and F_{ad} will be altered by different amounts, because of the difference between the primed and unprimed surface energies. As a consequence any conclusions about the work of separation drawn from measurements of the contact angle should be regarded as at best qualitative. As an example of the importance of oxygen, it has been observed that the same amount of copper forms larger clusters on a reduced alumina surface compared to an oxidized surface (Gota *et al* 1995). The plausible interpretation was a reduction in γ_{12} due to the formation of strong Cu–O bonds. Other complex examples have been discussed by Eustathopoulos and co-workers (Drevet *et al* 1993, Espie *et al* 1994, Eustathopoulos and Drevet 1994, Merlin and Eustathopoulos 1995).

For a theoretician, a direct calculation of θ or F_{ad} is problematic; the more straightforward thing to do is to calculate W_{sep}, by comparing the total energy of two systems, one in which the surfaces are free and the other in which they are in contact, forming the interface (figure 1). For the purpose of furnishing data which might help to explain mechanical properties, this is exactly what we want. However, when comparing with equilibrium data this approach has to be tempered with caution and an awareness of the segregation chemistry and thermodynamics in the system. If we are interested in predicting the dynamics of wetting for example, or the morphology of film growth, which are important for understanding supported metal catalysts, then the driving forces are provided by the difference between equilibrium (unprimed) and instantaneous values of the interfacial free energies and may not be closely correlated to W_{sep}.

3. Empirical correlations

Humenik and Kingery (1954) found that the wettability of oxides by liquid metals was an increasing function of the heat of formation of the oxide of the wetting metal. This theme has been developed since by many groups. For example the correlation between good wetting and reactivity of the metal has been observed in metals on oxidized W (Peden *et al* 1991). A large amount of data have since accumulated for metals on TiO_2 surfaces, particularly the (110) surface (Diebold *et al* 1995). This is because it is a stable surface which can be well characterized by LEED and photoemission spectroscopy (it is a semiconductor, which avoids the problems of surface charging) besides the fact that it is of great technological interest (Henrich and Cox 1994). For metals with a higher oxygen affinity (in the increasing order Cu, Fe, Cr, Hf), there is a tendency for the Ti to be reduced from its four-valent state and at the same time the wettability is higher. There appears to be no reduction of the Ti by Rh and metals to the right of Fe.

In a classic paper, which is still an excellent review of the subject, Naidich (1981) discussed the connection between wettability and chemical reactivity of liquid metal with a surface. He introduced the 'dynamic force of spreading', $F = \sigma_{lv}(\cos\theta_{equil} - \cos\theta_\tau)$ where θ_τ is the instantaneous wetting angle, thereby introducing the idea that we are often observing a snapshot of a system which is in a process of change rather than a thermodynamic equilibrium state.

Naidich distinguishes chemical wetting from physical wetting. Only the first, he claims, can provide the tens of kcal mol^{-1} necessary to give a work of adhesion comparable with the surface energies which are typically of order 1 J m^{-2} in metals. Physical wetting, which I do not think is relevant to metal–ceramic adhesion, is due to van der Waals interactions and is one or two orders of magnitude weaker. Chemical wetting includes the ionic kind of electrostatic force, as in the image interaction discussed below, which can be at least as large as forces derived from covalent bonds. Of course both are ultimately purely electrostatic, the difference being in the distribution of electron density.

Naidich further distinguishes equilibrium wetting from non-equilibrium wetting, the latter being the transitory situation during which a chemical reaction is taking place. The irreversible thermodynamics of non-equilibrium wetting is treated by taking account of the changes in chemical potential for formation of a new boundary phase. A number of important correlations were pointed out by Naidich:

- Wettability increases with the affinity of the liquid metal for oxygen, as mentioned above.
- There is a correlation between an oxide's electrical conductivity, the smallness of its free energy of formation and its wettability by a liquid metal.
- Thus the wettability is like the difference in free energy of formation of the oxides. He recognized that the non-equilibrium wettability is meant here.
- He gives several examples of how the addition of oxygen to the liquid metal improves the wetting.

Another useful general review with references on physics, chemistry and engineering of metal/ceramic interfaces is that of Howe (1993). He points out the strong positive correlation of wettability with ionicity in both oxides and carbides. Howe introduces a controversial point by suggesting that the interfacial energy also appears to depend not only on the interaction of the metal with the oxygen of the ceramic but also with the metallic component of the ceramic (the cations); this is indicated by the difference in the work of adhesion between Cu–ZrO_2 and Cu–SiO_2. Naidich on the other hand would interpret this

to mean that the wettability depends on the affinity of the components of the ceramic *with each other*. The unresolved issue here is how important are the direct interactions between the metal and the cations. Howe also points out a strong dependence of the wettability on stoichiometry; in one example, going from $UO_{2.001}$ to $UO_{2.084}$ caused a contact angle to decrease from 166° to 84° (Nicholas and Mortimer 1985).

Naidich suggested that the contact angle of a metal A on an oxide is reduced when a metal B is added to A such that B would reduce the oxide. This is borne out in some cases, for example for Cu, Ag, Sn and Ga on alumina, in which the addition of Ti steadily reduces the contact angles. It is not, however, a necessary condition, as Eustathopoulos and co-workers have shown (Eustathopoulos and Drevet 1994) by systematically studying the effect of various alloying additions. One suggestion is that there is a transition between wetting behaviour controlled by interfacial energy and wetting behaviour controlled by reaction energy—the chemical reaction of the metal with the substrate. There is a conceptual difficulty in treating interfacial energy and reaction energy as independent quantities, coupled with the problem that a chemically reacting interface is subject to steric constraints at the molecular level, which makes it difficult to estimate local relative free energies from bulk thermodynamic parameters. To really understand what is going on in these correlations, a more fundamental approach at the atomic scale is needed.

4. The image interaction

A point charge q is attracted to a metal surface by its image, which at a distance z gives rise to the classical image interaction:

$$E(z) = -q^2/4(z - z_0) \tag{4.1}$$

where z_0 is the position of the image plane. If ions are treated as point charges, equation (4.1) is the basis of a simple model of the adhesive energy between an ionic crystal and a metal surface. The idea has been introduced by Stoneham (1983) and co-workers (Finnis *et al* 1990, Duffy *et al* 1993, 1994, 1995) that this is in fact the dominant term in the adhesion of ionic crystals to metals. It has to be balanced by a short-ranged repulsive interaction. A back-of-envelope calculation shows that equation (4.1) indeed gives an adhesion energy in the order of joules per square metre. I will sketch here why the image model is at all a reasonable description of the quantum mechanical bonding across the interface; for further details the reader is referred to Finnis (1992).

It has sometimes been suggested that this classical formula includes only the electrostatic energy of the interaction, omitting some terms such as the change in kinetic energy of the electrons or terms vaguely referred to as 'chemical'. In fact it can be shown (Finnis 1992) that all these effects are implicitly included in the above classical image interaction, albeit within a simple level of approximation. That approximation consists in two parts; the truncation at second order of a perturbation series and an approximation to the response function. Firstly, the ceramic is replaced by an equivalent lattice of rare-gas atoms. For example MgO or AlN would be represented by neon gas. The interaction of this artificial rare gas with the metal is the zeroth-order approximation to our system. It is a repulsive interaction, which can be modelled by an effective-medium theory (Puska and Nieminen 1984) or purely empirically, and this is the first part of the approximation. The next step is to switch on the protons on those rare-gas atoms which are to be cations, and to switch off the protons on those that are to be anions. The rearrangement of electron density which accompanies this step could be calculated in principle by perturbation theory, as could the energy change. We stop at the first-order response of the metal, and approximate this by a

classical response function. This is the second part of the approximation. It gives a term in the interaction energy within the second order of perturbation theory. In the discrete classical model (DCM) of Finnis (1991), the classical response function treats the discrete nature of the metal lattice by regarding it as an assembly of charged conducting spheres, the electrostatic potential of which is constant. Only dipole polarizations are allowed, besides the charge transfers between the spheres. The discrete treatment of the metal atoms makes a difference to previous image models, which regarded the metal as a semi-infinite continuum.

The DCM has so far been tested simply for a point charge above an aluminium surface (Finnis *et al* 1995), giving good agreement with *ab initio* calculations in its qualitative description of the corrugations on the (110), (100) and (111) surfaces as well as the asymptotic image behaviour. Its quantitative testing for an ionic solid in contact with a metal is a subject of current research. An interesting consequence of the assumption that the image interaction is the dominant term in the adhesion is the implication that it depends on self-consistency of the electron density with the perturbing potential. Perhaps another starting point can be employed which avoids this consequence; otherwise there is no escape in an electronic structure calculation from iterating the calculation to self-consistency.

A model of the work of separation such as this is not a complete theory. For one thing, it does not say anything about the electronic structure—the local densities of states and charge density. It is also necessary to fit the parameters in the image model to self-consistent first-principles calculations which are parameter free, or *ab initio*. Such calculations are now available for some systems, and the main results will be described later in this article. First I will describe some general features and trends which have been obtained by less rigorous methods.

5. Studies of trends

5.1. The electronic structure

Noguera and Bordier (1994) (NB) have approached the understanding of bonding between metal and oxide with a simple quantum mechanical model of each system. Their model illustrates some of the important qualitative ideas in these systems, so I shall discuss it in the following. It is similar to the model of the metal–semiconductor junction introduced by Heine (1965). They treat the metal as a jellium, whose eigenstates are plane waves. The oxide is treated as a tight-binding system with one s orbital per site. The local orbitals have self-energy ε_A on the anions and ε_C on the cations, and are coupled between nearest neighbours by the isotropic overlap integral β. Both rock-salt and zinc-blende structures were considered. Within this model the band gap in the oxide is $\varepsilon_C - \varepsilon_A$ and a measure of the ionicity is $(\varepsilon_C - \varepsilon_A)/\beta$, which varies from 0 (purely covalent) to infinity (purely ionic). The plane waves are matched onto the local orbitals at an abrupt interface.

There are no strictly localized states at the interface. At energies within the band gap, the states which within the metal resemble plane waves become evanescent functions when they enter the oxide, decaying roughly exponentially with distance into the oxide over a typical length l_p. Within this energy range they are referred to as MIGS (metal-induced gap states) and are a general feature of metal–ceramic interfaces. Their decay length l_p for different materials parameters was calculated by NB and increases as the band gap decreases. As pointed out by NB, the MIGS deplete the oxide density of states above and below the band gap. For near the bottom of the gap they are built from a large proportion of valence band-like states and near the top of the gap they are built from a large proportion of conduction band-like states. NB define a certain energy called the zero-charge point,

E_{ZCP}, which is the energy below which there are the same number of states as when the metal was not present. In a detailed model this would be a function of position near the interface. Its significance lies in its position relative to the Fermi energy of the metal, E_F. If the MIGS are occupied just up to energy E_{ZCP}, there is no net charge transfer to the ceramic compared to its neutral value. The neutral value means here the charge states of the ions as they appear in the bulk oxide, which is close to $2-$ for oxygen and $3+$ for Al.

The assignment of charges to ions should not be interpreted as very precise because it is not unique. The allocation depends on the particular choice of atom-centred basis functions. It is nevertheless a common way of describing the results of tight-binding or other calculations which use a basis of atom-centred orbitals. The usual way of calculating the charge on an ion is by a Mulliken population analysis of the wave functions, which for bulk alumina indicates a charge on the oxygen ions of 1.75–1.83, depending on convention (Ching and Xu 1994). The O^{2-} ion seems to be fairly robust to changes in the local environment. If for example E_F were above E_{ZCP}, a transfer of electrons from the metal to the ceramic would take place, creating an interface dipole which induces a relative shift of the bands. In a semiconductor a gradual bending of the bands would be the result of the more spread out nature of the dipole layer. For a large-band-gap oxide, there is hardly any transfer of electrons; NB find typically a few hundredths of an electron are transferred per interfacial atom.

The charge transfer is small enough that, even though the density of MIGS is low, the Fermi level stays fairly close to E_{ZCP}. Anticipating the results to be described later, it is remarkable that for three diverse systems, Ag, Ti and Al on MgO(100), the Fermi level predicted by self-consistent first-principles calculations is 2.0–2.2 eV above the top of the valence band in each case. For Nb on $Al_2O_3(0001)$, the Fermi level is predicted to be 3 eV above the top of the valence band.

5.2. Cluster calculations

A seminal set of calculations was made by Johnson and Pepper (1982), who used a self-consistent scattered-wave approach. This is an *ab initio* electronic structure method, albeit not as accurate as the methods to be discussed later, and not suited to calculation of total energies. They discuss the states of a single transition metal atom (Fe, Ni, Cu and Ag) in contact with a cluster of AlO_6, chosen to represent a sapphire surface. An extra nine electrons were provided in the system to ensure that the oxygens would be in the expected O^{2-} configuration. These calculations opened the perspective of understanding the nature of the bonding between metal and oxide on a quantum chemistry basis.

The atomic d orbitals of the added metal atom were seen to hybridize with the oxygen p orbitals in the upper valence band, producing bonding states and antibonding states. The bonding states were fully occupied, whereas the antibonding states were partially occupied for Fe and Ni, and fully occupied for Cu and Au. There was a partial charge transfer from metal to oxide ion, also decreasing in the sequence Fe, Ni, Cu, Ag. These two effects were invoked to explain the trend in measured metal–sapphire contact strengths in terms of the energies of the occupied one-electron orbitals and the charge transfer, which decreased in the same sequence.

By the standards of modern *ab initio* calculations, these results are only qualitative, and in particular Johnson and Pepper's use of a charged cluster of seven atoms of oxide against one atom of metal is a severe approximation to an interface, which cannot deal with the questions of band shifting described above. Nevertheless the formation of bonding and antibonding states between d and p orbitals and the transfer of charge from the metal to the

oxide remain valid effects; one would like to know in more detail how they vary with the thickness of the metal on the oxide, and how predictive the whole theory can be made. The first steps in this direction are described in the following sections. Semi-empirical methods such as tight binding remain of interest here in order to provide interpretation of more exact model calculations, and because they can handle more atoms.

A semi-empirical atomic orbital method was used by Nath and Anderson (1989) to re-examine the conclusions of Johnson and Pepper in more detail, and to make an estimate of the adhesion energy. They used a larger cluster of $(Al_4O_{18})^{15-}$. This cluster is a sandwich of Al between two terminating (0001) surfaces of O, and carries nine holes in the valence band of O 2p orbitals. With this choice of electron number, the unfilled band mimics the O^- state which surface oxygen ions on a semi-infinite slab would have to have in order to satisfy overall charge neutrality. They could then naturally be reduced to O^{2-} by the metal slabs with which they were brought into contact. These metal slabs comprised two layers of 31 or 29 atoms. The 3d transition metals were examined from Sc through to Cu. The binding energies to the oxygen-rich alumina varied from 5.3 eV per interfacial O for Sc to 0.81 eV for Cu. The picture of Johnson and Pepper was broadly confirmed, but with the additional feature that a covalent stabilization of the O 2s orbitals contributed to the bonding to an extent which decreased towards Cu, because of decreasing orbital overlap. Nath and Anderson pointed out on the basis of their large values of the work of separation that the cleavage of a metal from the surface would more likely take place between the terminating metal plane and the next plane of metal, rather than between the oxygen plane and the metal. The same conclusion was reached on the basis of *ab initio* calculations for an extended system by Kruse *et al* for the case of Nb–Al_2O_3, as described later.

Although calculations for small clusters are helpful, the problem of locating excess charges and making the calculations representative of bulk material is a serious one, which only really goes away when a sufficient number of metal layers are included to screen the interface. Thus the cluster methods have been strongly challenged by supercell calculations using a repeating infinite-slab geometry.

5.3. Semi-empirical slab calculations

With an extended Hückel model, equivalent to the tight-binding description (Hoffmann 1988), Alemany and co-workers studied the electronic structure and adhesion of the first-row transition metals to idealized surfaces of Al_2O_3 (Alemany *et al* 1993) and AlN (Alemany 1994) .They generally confirmed the picture of Nath and Anderson described above. Unlike Nath and Anderson, however, they found no significant O 2s contribution to the bonding. These calculations still neglect self-consistency with respect to charge transfer and all effects of the Coulomb potential associated with charge transfer. For this reason no Coulomb dipole could be induced at the interfaces, and the Fermi energy remains at its value for the bulk metals, several eV higher with respect to the top of the valence band than in *ab initio* self-consistent calculations. These authors also calculated the work of separation under various assumptions for the surface termination. The results are very sensitive to the assumptions. For example, for one of the strongest adhering metals, V, a value of about zero was found for the work of separation to a {0001} surface of neutral O atoms (representing a positively charged surface in the ionic picture, because the Al^{3+} in the subsurface layer are not compensated in this case), which became a huge 18 J m^{-2} when three holes were introduced into the O 2p band, which represents a neutral surface in the ionic picture. The work of separation was correlated to the Fermi energy, going down in magnitude across the transition series, but rising again with the Fermi energy at Cu.

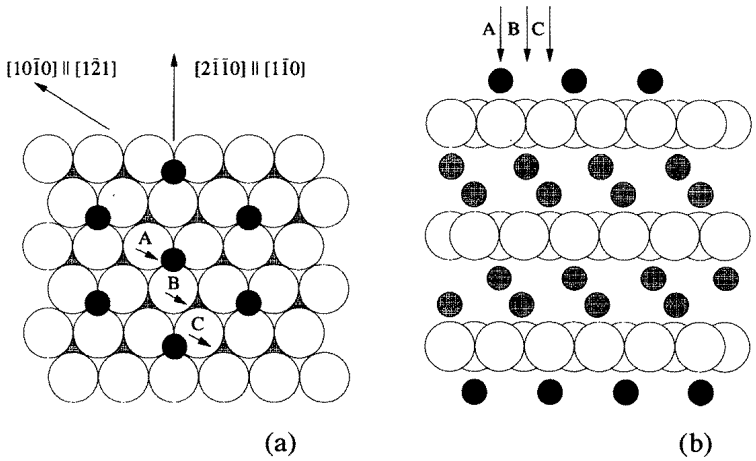

Figure 3. The three sites on a basal plane of α-Al_2O_3 described in the text.

The tight-binding calculations of Kohyama and co-workers (Yamamoto *et al* 1989, Kohyama *et al* 1990, Ohuchi and Kohyama 1991, Kohyama *et al* 1992) included on-site terms in the d block of the Hamiltonian on the Nb atoms which varied linearly in proportion to the charge on the site. This is the simplest form of self-consistency. They studied the series of 3d and 4d transition metals on Al_2O_3 and AlN. These authors have studied especially thoroughly the system Nb on Al_2O_3{0001}. They included 1/3, 2/3, 1 and 2 monolayers of metal on the surface. This is a natural way to build up a metal layer, with the convention that the stoichiometric (0001) surface is terminated by 1/3 of a monolayer of Al. Between the Al atoms on the stoichiometric surface, which occupy sites A, there are an equal number of sites B and sites C (see figure 3). Occupancy of A, B and C completes the monolayer according to this definition of a monolayer. Confusion is possible here, because while this configuration mimics a close-packed plane of Nb in contact with the oxide, which is believed to be the thermodynamically most stable situation, in specimens grown by molecular beam epitaxy (MBE) as studied by Mayer and co-workers, the layers of Nb which grow are {111} and each occupies only 1/3 of a monolayer in the above sense.

These calculations also confirm the qualitative picture from the clusters, in which there is a progression of the Fermi energy from bonding states at the bottom of the d band to antibonding states at the top in going across the transition series from Zr to Pd. The monolayer calculations do not show a fully developed d band, but when the second layer of Nb is added the d band becomes very bulk-like. In all these calculations the position of the Fermi energy is about 5–7 eV above the top of the valence (O 2p) band of the Al_2O_3, while the centre of the d band moves downwards as the d band fills. Again, there is no long-ranged Coulomb interaction in these calculations which would cause a dipole layer to develop, and this may account for the 3–4 eV higher position of the d band in Nb compared to the self-consistent calculations of Kruse *et al* (Kruse 1994, Kruse *et al* 1996). Kohyama and co-workers emphasized that their method should not be expected to give quantitative results, because of the lack of full self-consistency, and the use of unrelaxed atomic positions. Indeed, for these reasons they did not attempt to calculate a work of separation.

6. *Ab initio* calculations

The first people to make a first-principles (sometimes called *ab initio*, in the sense that no parameters are empirically determined) density functional calculation of the adhesion of a metal to an ionic crystal were probably Gubanov and Dunaevskii in 1976 (Gubanov and Dunaevskii 1977). They represented the metal as a jellium surface, the electron density of which was corrugated by the external potential due to the ionic crystal, treated as a half-space of point ions. The ionic charge densities were treated as constant spherical clouds, rigidly superimposed. The Thomas–Fermi model with gradient corrections (see, for example, Lundqvist and March 1983) was used to describe the kinetic energy of the electrons. These authors included two variational parameters in order to describe the amplitude and decay of the induced corrugations, with which they minimized the total energy. This enabled them to calculated plausible values for the equilibrium separation and work of adhesion within their model for various metal–ionic crystal pairs. Nowadays one can criticize the quantitative accuracy of this calculation; the TFDW functional and the jellium model are known to be very poor for describing the surface energy of aluminium, giving a negative answer; nevertheless, the essential physics of the adhesion is probably captured in their calculation, which includes for example the image interaction. However, just like the classical image model of metal–ceramic adhesion, this approach still gives no information about the electronic states.

More recently, *ab initio* density functional calculations which use the local density approximation (LDA) for exchange and correlation but not for kinetic energy have been applied to several oxide–metal interfaces. One has to solve the Kohn–Sham equations (Kohn and Sham 1965), in which an effective potential for independent particles V_{eff} represents the electron–nucleus and the electron–electron interactions, including exchange and correlation:

$$-\nabla^2\psi_i(\boldsymbol{r}) + V_{eff}(\boldsymbol{r})\psi_i(\boldsymbol{r}) = \varepsilon_i\psi_i(\boldsymbol{r}). \tag{6.1}$$

In the LDA, the part of $V_{eff}(\boldsymbol{r})$ which represents exchange and correlation is a function only of the local density of electrons, which in the self-consistent solution is given by

$$n(\boldsymbol{r}) = 2\sum_{\varepsilon_i \leqslant \varepsilon_F} |\psi_i(\boldsymbol{r})|^2 \tag{6.2}$$

in which the summation runs over occupied states, i.e. those with energy below the Fermi energy ε_F. These equations are solved self-consistently, and the total energy of the system is obtained. The single-particle energies ε_i are also often interpreted as the band-structure, although this really goes beyond the scope of the LDA. Details of the theory and the many ways in which it is implemented can be found in the literature (Jones and Gunnarsson 1989) and need not be repeated here. Suffice it to say that it has been extraordinarily successful as a method of total energy calculation, and can also reproduce measured work functions and Schottky barriers. It requires extension for magnetic systems, the most simple extension being the local spin-density (LSD) approximation, in which densities for up and down spins are treated as separate, with spin-dependent contributions to the effective potential. The most serious shortcomings of the LDA or LSD are seen in metals and oxides to the right of the transition series, where correlation effects are decisive, and in the band gaps of semiconductors, which are always predicted to be too small, so a 'band-gap correction' has to be applied.

A case in point is SiC. Lambrecht and Segall (1992) have studied the electronic structure and energy of interfaces between SiC and TiC. This may be the most important interface to study when Ti is brought into contact with SiC. The band gap of SiC in their LDA

calculation is 1.4 eV, which is about 1 eV less than the experimental estimate. At this interface an important occupied bonding state, resulting from overlap of Si dangling bonds and Ti 3d t_{2g} orbitals, appears just above the bottom of the LDA conduction band in SiC; hence there is considerable band bending. It is suggested that in an a more accurate calculation going beyond LDA this bonding state would lie in the gap. The argument is based on the observation that LDA calculations of semiconductor band offsets give results in good agreement with experiment; therefore the band-gap correction should mainly affect the bottom of the conduction band, or the unoccupied states. The gap state should carry a proportion of this correction, but not all. Clearly there is still uncertainty about the electronic structure of interfaces of this type, although by analogy with bulk materials, the calculated total energies are probably more reliable.

While the LDA always underestimates band gaps (when the ε_i are interpreted as the real energy levels), it fails to predict any gap at all in the notorious example of NiO. In NiO and similar oxides the *ab initio* method of choice is based on the Hartree–Fock equations, to which a correction may be added for the correlation energy. This is unfortunately a much more costly method from the computational point of view than the LDA method, which itself requires orders of magnitude more computer time than the semi-empirical approaches. At least for the most studied oxides MgO and Al_2O_3, the LDA and Hartree–Fock methods appear to be in good agreement, so both are probably valid. Some kind of *ab initio* method on an extended system is necessary for quantitative information, although just how quantitative that information currently is remains uncertain. Less computationally intensive semi-empirical models remain useful for studying trends.

7. The Ag/MgO interface

The most effort in *ab initio* quantum mechanical calculation has been devoted to the Ag/{100}MgO interface, because of its simplicity. It is a non-reactive interface, with only a 3% misfit in the lattice parameters. That is to say, the cubic lattice parameter a_{MgO} is 3% larger than a_{Ag}. As a result, it was possible to prepare planar regions of coherent interface by molecular beam epitaxy and they were imaged in the high-resolution electron microscope (Trampert *et al* 1992). The images showed also the presence of periodic misfit dislocations. Their spacing (6.53 ± 1.02 nm) and $\langle 100 \rangle$ orientation were consistent with the existence of a square network of $\langle 100 \rangle$ edge dislocations with Burgers vector $1/2a_{Ag}\langle 100 \rangle$, which would be appropriate for relieving the misfit strain. The interpretation is that these are partial dislocations, which separate two kinds of coherent region to form a chequerboard pattern. On one set of squares of the chequerboard Ag atoms are vertically above O atoms (figure 4, site B) and on the alternate squares they are above Mg atoms (figure 4, site A). From the measured contact angle for islands of Ag on the surface, $F_{ad} = 0.45 \pm 0.1$ J m^{-2}. On the assumption that the MgO surface is stoichiometric, and the Ag surface uncontaminated, which is reasonable in the UHV conditions of preparation, then $F_{ad} = W_{sep}$. The interpretation of this number is tricky if indeed the interface is actually a chequerboard of B and C interfaces. One is presumably measuring an average value of F_{ad} for these interfaces, but reduced by the energy of the misfit dislocations.

In apparent contradiction to this picture of the geometry, Guénard *et al* (1994) found an array of $\langle 110 \rangle$ dislocations spaced at 9.5 nm in a similar sample, using grazing-incidence x-ray diffraction. This would indicate that only one type of interface need be present, since the dislocations are not partial. As a possible explanation of the discrepancy, these authors suggested that a transformation in the geometry might have taken place in the sample of Trampert *et al* while it was at a temperature above 50 °C, perhaps when the transition from

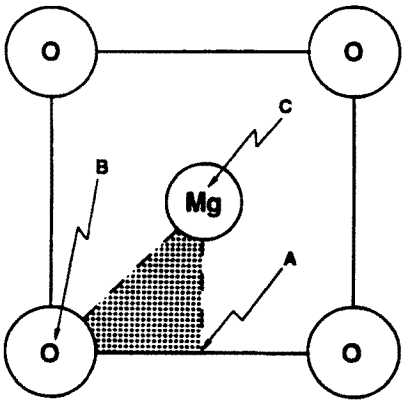

Figure 4. The three sites on a {100} plane of MgO described in the text.

a two-dimensional to an island structure takes place.

At least two groups have made *ab initio* calculations for the monolayer of Ag on MgO. Using the full potential linear augmented plane-wave (FLAPW) method, a fully self-consistent implementation of LDA, Li *et al* (1993) found the stablest configuration to be Ag on O (site B), with a spacing of 0.27 nm. This agrees well with the Hartree–Fock calculation (corrected for correlation) of Heifets *et al* (1994), who found a spacing of 0.26 nm, although the adhesion energy is somewhat different (table 1). Very little charge transfer was found between the Ag and the surface layer.

Schönberger *et al* (1992) calculated the full metal–ceramic interface in a slab geometry, in which the oxide was represented by three layers of MgO and the metal by three layers of Ag, with periodic boundary conditions in all three directions. They used the full potential linear muffin-tin orbital (FP-LMTO) method, which like the FLAPW is one of the most accurate LDA methods. The result was again that the Ag on O position B had the lowest energy (table 1), followed by the hollow site A, then the Ag on Mg C position. These authors varied the spacing of the planes between metal and oxide and within the metal in order to minimize the total energy. The Ag–O spacing at minimum energy was 0.25 nm, just slightly less than the previous monolayer calculations. The relatively high value (1.59 J m^{-2}) of the work of separation is puzzling. The oxide surface energy which is a part of this calculation (1.8 J m^{-2}) is also relatively high compared to the monolayer calculations and to an estimate from experiment (see Schönberger *et al* 1992) of around 1.1 J m^{-2}. If one were to take the latter number as correct, the estimated work of separation would come down to 0.9 J m^{-2}, which is more in line with the monolayer calculations. A similar calculation was made by Hong *et al* (1994), using a self-consistent method based on local atomic orbitals expanded in Gaussians. Their work of separation is similarly high (1.8 J m^{-2}) and the Ag–O bond length (0.235 nm) is just slightly less than that of Schönberger *et al*.

A further good reason for the theoretical W_{sep} to exceed the experimental estimate is that in the experimental sample there are misfit dislocations, whose energy reduces the adhesion by the product of the dislocation density per unit area times the line energy of the dislocations. It is not easy to make a reliable estimate of the line energy of misfit dislocations, since the unit cells required in order to include one are still too large for *ab initio* methods, and a reliable energy functional for quantitative semi-empirical calculations is not yet available. A crude estimate can be made if we assume that their energy is not

dependent on the substrate, provided the dislocations are localized, in which case we can extract their energy from the embedded-atom calculations for Ag on Ni which included misfit dislocations (Gumbsch *et al* 1991). The result amounts to 0.09 m J m^{-2}, suggesting that the energy of misfit dislocations is not the major source of discrepancy.

Table 1. The calculated work of separation (adhesion) for Ag/{100}MgO, J m^{-2}, for the three sites indicated in figure 4. The first two sets of calculations are for a monolayer only.

Authors	Mg (site C)	O (site B)	Hollow (site A)
Heifets *et al* (1994)	0.63	0.81	0.74
Li *et al* (1993)	0.54		
Hong *et al* (1994)	1.08	1.9	
Schönberger *et al* (1992)	0.7	1.6	1.1
Experiment (Trampert *et al* 1992)		0.45	

These calculations give detailed information about the electronic structure, which we illustrate from the calculations of Schönberger *et al*.

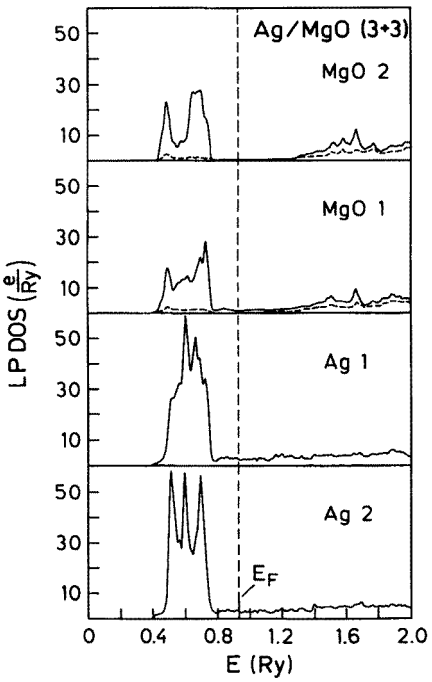

Figure 5. The layer projected density of states for the Ag/MgO interface (Schönberger *et al* 1992).

Figure 5 shows the layer projected density of states (LPDOS) for each layer of atoms in the Ag/MgO system. The main hump in the Ag LPDOS is the contribution of the full d

band, on top of which there is a much lower density of states up through the Fermi energy, mainly composed of the s and p atomic states. The d band closely matches in energy the upper valence band of states in MgO which is mainly composed of oxygen 2p orbitals. At the interface these bands hybridize to some extent, but the resulting bonding, non-bonding and antibonding orbitals are full and this process cannot contribute to the adhesion. This must be due to more subtle interactions between the orbitals and potential on the Mg and O with those on the Ag. The classical image picture on the other hand has no problem with explaining the adhesion. In this picture there is a surface-induced charge density on the metal which oscillates in sign in antiphase to the charges on the ions and which attracts them.

On the question of site preference, we might expect from the image model that above O would be the favoured site for Ag, for the following reasons. The image interaction with rigid anions and cations would predict the same attraction for Ag atoms above O as above Mg. However, the greater polarizability of the O ion would further lower the electrostatic energy when Ag is above it. Plausible as this argument may seem it is not really good enough, because the final adhesion energy also depends sensitively on the model used for the short-range repulsion (Duffy *et al* 1994). Presumably the repulsion is stronger for Ag–O than Ag–Mg. The repulsive term may also be the cause of the puzzling *ab initio* result that the hollow site is more attractive to Ag than the Mg site. It is puzzling, because in the DCM, with Ag above the hollow site there would be precisely zero attraction by symmetry.

We see in the LPDOS of the interfacial MgO layer that there is the expected small density of states throughout the gap in this layer, which becomes negligible at the depth of the second layer. This is due to the tails of the metallic states referred to in subsection 5.1, and a small density like this would of course exist even in the absence of any ceramic.

Before leaving the subject of Ag/MgO it is worth noting that the thermodynamically stable interface is apparently formed by MgO{111} planes, as deduced from the octahedral shape of MgO particles in cube-on-cube orientation to Ag observed after internal oxidation of Mg in Ag (Mader and Maier 1990). At first this was surprising, because the stable free surfaces of MgO are {100}. A {111} surface plane would be charged if the ions had their normal valence and there were no missing atoms, and a charged surface has a divergent electrostatic energy. These two reasons combined explain why free {111} surfaces are not expected. However, because a sharply terminated MgO{111} plane of ions has a net charge, it will induce a compensating image charge in the metal with which it will bond strongly. In principle the bounding 111 plane of MgO might be of either Mg or O, but the evidence points to it being oxygen (Mader and Maier 1990). As these authors discuss, the {111} interface appears to be common to other metal–MgO pairs even when there is a large misfit. *Ab initio* calculations of this interface would be interesting and perfectly feasible. Whether or not the bounding plane is of O or Mg is not easy to predict, and it depends on the oxygen partial pressure.

8. The Ti/MgO and Al/MgO interfaces

Schönberger *et al* (1992) made similar calculations for the Ti/MgO system, which provides an interesting comparison with Ag/MgO, since Ag is a metal with a full d band, whereas the d band of Ti is only partially occupied. Ag and Ti have similar atomic volumes, so it is also a system in which a coherent interface is a reasonable approximation. The Ti above O geometry was assumed, and again the energy was minimized with respect to the interlayer spacing at the interface. Unfortunately it has not been possible experimentally to make a specimen of this system. Five layers each of Ti and MgO were used, and the

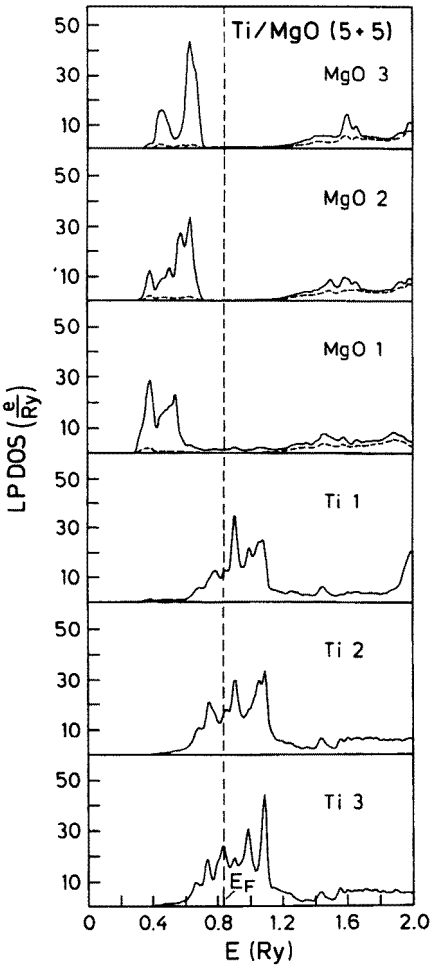

Figure 6. The layer projected density of states for the Ti/MgO interface (Schönberger *et al* 1992).

LPDOS is reproduced in figure 6. In this case there are clear signs of hybridization of the d band of Ti with the O 2p band. Notice the large bonding peak at the bottom of the valence band in the first MgO layer. The peak in the centre of the d band which is strongest at the interface is not a hybridization effect but is also a feature of the free surface. Although the Fermi energy is now just below the middle of the d band of Ti, it still lies about the same distance above the valence band in MgO, as discussed previously. Now however there are unoccupied antibonding states from the d–p hybridization; we expect the adhesion to be stronger than for Ag and it is. The calculated work of separation is 2.2 J m^{-2} compared to 1.6 J m^{-2} for Ag/MgO.

In a similar way to their Ag/MgO calculation, the Al/MgO interface was treated by Hong *et al* (1994) with the self-consistent method with an atom-centred Gaussian basis. In this case, although we cannot make a direct comparison with experiment, it is of great interest to study how a simple s–p-bonded metal like Al interacts with the oxide. Again the

Fermi energy in the nearly free-electron-like band of Al lies about 2 eV above the valence band of MgO, as for the other metals. Like Ag, Al prefers to sit above the O sites rather than the Mg sites. Compared to Ag, the work of separation of Al from the MgO surface is less by 0.4 J m^{-2} (see table 2).

Table 2. The calculated work of separation W_{sep} (mJ m^{-2}) and equilibrium Al–MgO spacing d_0 (nm) for five layers of Al above O (site B) and above Mg (site C), after Hong *et al* (1994).

	Site B	Site C
W_{sep}	1.10	0.24
d_0	0.213	0.316

Hong *et al* pointed out that the difference in the calculated work of separation between Ag and Al can be attributed to the difference in the surface energies of the metals. It is about the same value (0.4 mJ m^{-2}) for site B and site C; by comparison the surface energy of Ag exceeds that of Al by 0.5 mJ m^{-2}.

Another interesting feature revealed by the calculations of Hong *et al* is that for both Al and Ag on MgO there is a charge redistribution of exactly the type one would expect from the image theory, namely a depletion of electrons on the metal atoms adjacent to O and a piling up of electrons on the metal atoms adjacent to Mg (see figure 2 of their paper). The image calculations for a metal surface in an external field showed that the induced charge is located outside the surface layer of metal atoms, and analogously here the induced charge is mainly between the metal and the first oxide layer.

9. The Nb/Al_2O_3 interface

The Nb/Al_2O_3 is an interface which bonds strongly without chemically reacting and which has been investigated intensively from the point of view of both atomistic structure (Mader 1989, Mader and Rühle 1989, Mayer *et al* 1990, Knauss and Mader 1991, Mayer *et al* 1992, Gutekunst *et al* 1994) and mechanical properties (Elssner *et al* 1994). The simplest interfacial structure is the one which appears when Nb is grown on α-Al_2O_3{0001} by MBE. The surface normal in Al_2O_3 is a threefold axis of symmetry, which is preserved at the interface because the interface plane of Nb happens to be {111}. The mismatch in lattice spacing in this orientation is less than 2%, and it is accommodated by misfit dislocations which Mayer and co-workers have observed in high-resolution transmission electron microscopy. The coherent interface is therefore also an excellent subject for theoretical study with a periodic slab supercell. The interpretation of the geometry of this interface was that the Al_2O_3 is terminated by an oxygen plane and that the first and second {111} layers of Nb approximately continue the Al sublattice.

Ab initio calculations have been made for this system using the pseudopotential method and a basis of plane waves (Kruse 1994, Kruse *et al* 1994, 1996). A slab of three layers of Al_2O_3 with periodic boundary conditions was used, as in previous calculations for the clean surface (Manassidis *et al* 1993). The electronic structure and total energy was calculated initially for a monolayer of Nb, in positions A, B or C (figure 3) on the oxygen-terminated surface. This layer of Nb replaces a layer of the same number of Al atoms in the stoichiometric surface. Space of equal thickness to the total of three Al_2O_3 layers was allowed between the periodically repeating slabs. The pseudopotential method allowed the forces on each ion to be calculated and the ions were all relaxed to minimize the energy. The

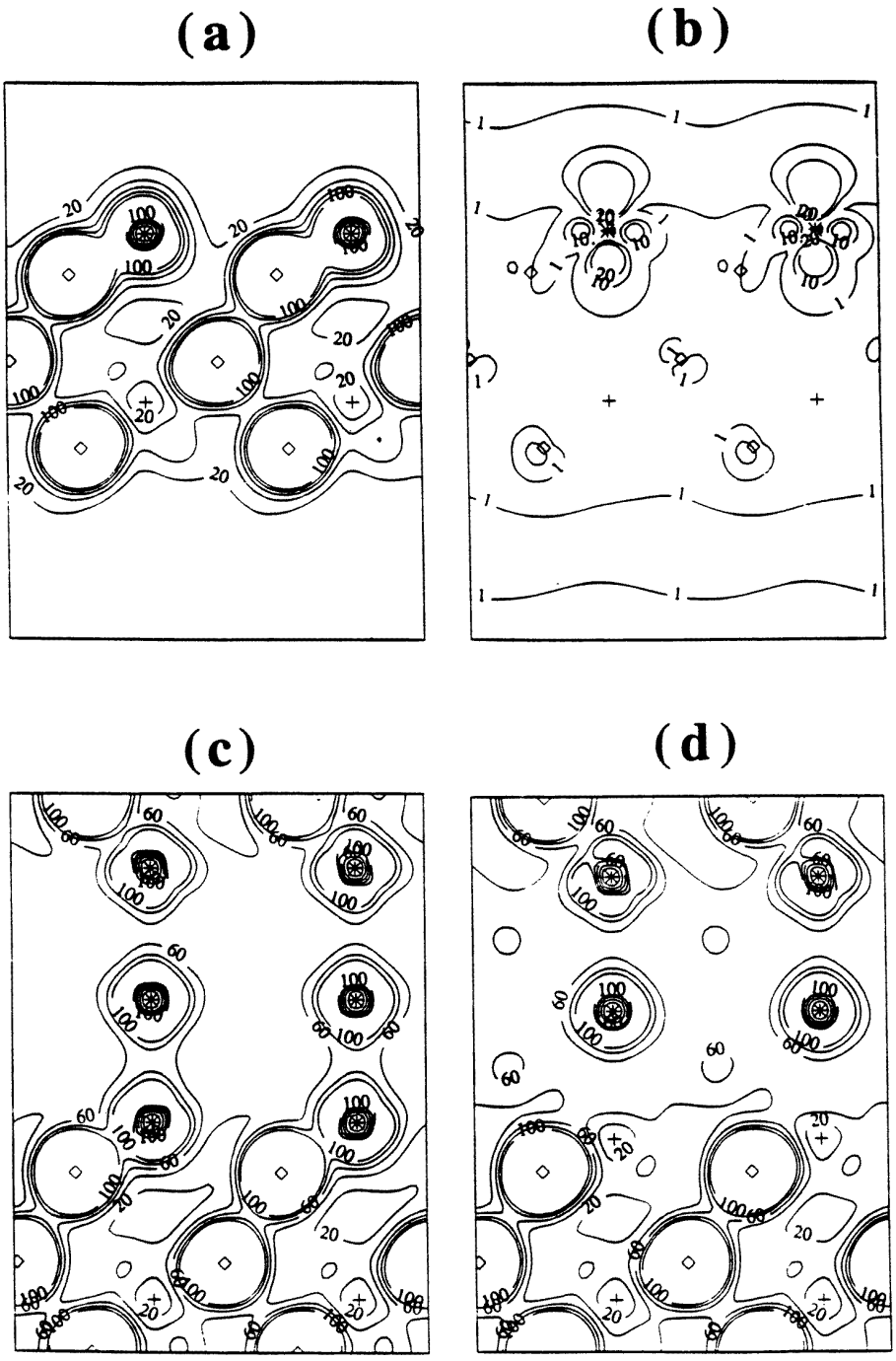

Figure 7. Self-consistent valence charge density on a $(\bar{1}100)$ section of the α-Al_2O_3 slab. Contours are separated by $3e^-$ nm^{-3}. $* = $ Nb, $\diamond = $ O, $+ = $ Al. (a) With a monolayer of Nb on sites A. The section is through a Nb–O bond. (b) The contribution of the highest occupied orbital to (a) at the Γ point. (c) For the case of eight layers of Nb filling the space between sapphire slabs. (d) For the case of Al-terminated α-Al_2O_3 and six layers of Nb.

extent of the relaxation and the total energy were both least in the case when Nb occupies the vacant Al sites, as it does in the experimentally observed interface. The explanation is simple: the Nb atom has given up three electrons to the surface O, which thereby become O^{2-}. The Nb^{3+} ion is then attracted by the empty octahedral site immediately below position A, whereas in positions B or C it is repelled by the Al^{3+} immediately below it. The total valence charge density, plotted in figure 7(a), does not reveal the ionic nature of the bond. We can see the ionic character clearly however in the charge density for individual bands. The highest occupied orbital then appears as a well localized, doubly occupied Nb 4d state (figure 7(b)), and there is very little overlap of any occupied orbital with both Nb and O sites. The occupied 4d state is of $3z^2 - r^2$ character, pointing out of the surface, so the Nb ion is very non-spherical. Features like this are a challenge to improve the tight-binding description of transition metal–oxide bonding, which up to now has dealt with spherical ions.

The bulk Nb–Al_2O_3 interface was simulated by filling the remaining vacuum with six layers of Nb. As a variant on this, in a separate calculation the Nb layer at the interface was replaced with Al, restoring the stoichiometry of the interface, which is now terminated by Nb–Al. There is relaxation between the Nb layers, which is significant in the case of the Nb–O-terminated interface. In this case the Nb at the interface is 0.114 nm from the oxygen plane, compared to 0.096 nm in the monolayer and 0.84 unrelaxed. At the same time the second plane of Nb relaxes towards the interface, so the spacing between the first and the second layers of Nb at the interface is reduced from 0.095 nm (bulk value) to 0.055 nm. Charge densities are illustrated in figures 7(c) and 7(d). Image simulation has shown that the Nb–Al and Nb–O interfaces might just be distinguishable by HRTEM (Möbus 1995) or a Fresnel technique (Stobbs 1995), but the experimental data have not yet achieved this level of resolution. A further step which needs to be taken at this point to verify the calculations against experiment is to perform more accurate image simulations by using the self-consistently determined electron density and potential, rather than the usual superposition of atomic charge densities.

The layer projected densities of electron states (figure 8) show significant interaction between the Nb orbitals and the O 2p, and there is no longer a clear picture of an ionic bond which was seen for the monolayer. The strong peak in the Nb density of states just above the Fermi level is probably a surface state rather than an antibonding state resulting from the interaction, but there is certainly overlap in the O 2p and Nb 4d states below the Fermi level.

10. Other metal/ceramic interfaces

Unrelaxed *ab initio* calculations for monolayers of Cu on Al_2O_3 and on AlN were made by Kasowski and co-workers (Kasowski and Ohuchi 1988, Kasowski *et al* 1988), in which they also made contact with experimental ultraviolet photoemission spectra (UPS). These calculations were made with two and four layers respectively of stoichiometric Al_2O_3 and AlN in a periodic geometry. The assumption of Cu–O bonds led to a better fit to the UPS than placing the Cu above Al, as we might have expected. Surprisingly however, it was significantly more favourable in energy to situate Cu above Al and to form Cu–Al bonds, than for the Cu to bond to N. This lower-energy solution was also in better agreement with the UPS. In the latter case the Cu d orbitals were mixed in with the valence band of the AlN.

There have been far fewer calculations for real metal–ceramic interfaces in which the ceramic is not an oxide. An interesting case is Ti on SiC, for which large non-self-consistent

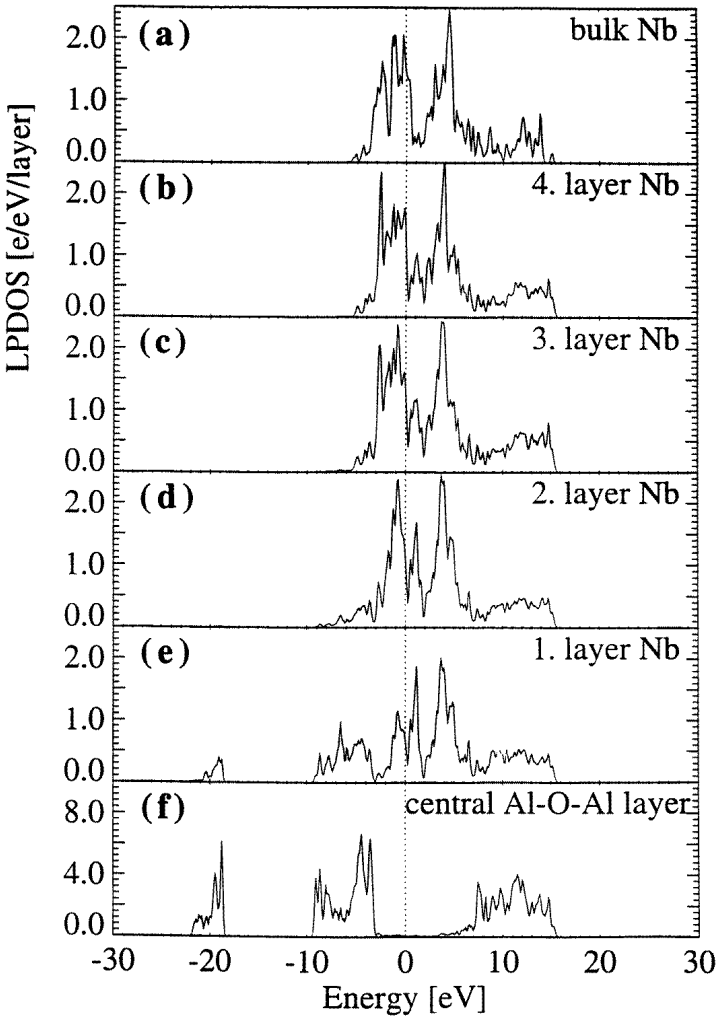

Figure 8. (a) The density of states in bulk Nb. (b)–(e) The layer projected densities of states on each Nb layer in the eight-layer slab, from the fourth down to the surface (adjacent to oxygen). (f) The density of states projected onto the central Al–O–Al layer of the slab with eight Nb layers.

cluster calculations were made by Mehandru and Anderson (1991). They looked at polar and non-polar (stoichiometric) interfaces to Ti(0001), finding that the binding was stronger to the polar interfaces, as we would also expect from image arguments in the case of an ionic material. In this case it was attributed to s–p-hybridized dangling bonds on the C- or Si-terminated surface, which combine with the Ti 3d orbitals. Earlier calculations of Al and Ti on SiC were made by Li *et al* (1988) and Mehandru and Anderson (1991). The problems of non-self-consistent calculations have been referred to, but it should be pointed out that although it has weaknesses, a semi-empirical quantum mechanical method can at least be made to give the correct band gap and so to sidestep the problem of the LDA mentioned above.

11. The effect of impurities

Trace elements, present in bulk to a few parts per million, such as sulphur or yttrium, can have a dramatic effect on the adhesive property of an oxide film. Yttrium in particular is well known to improve the adherence of the oxide (the reactive element effect, or RE effect as it is known) which is crucial to the performance of components at high temperature in gas turbines. This has motivated theoretical calculations of impurity effects on the bonding at the interface.

Anderson and colleagues (Anderson *et al* 1985) calculated the adherence of alumina on Ni–Al alloys with and without the presence of Y. These authors used a non-self-consistent tight-binding model Hamiltonian, with clusters to model the metal and oxide. A similar model was used by Hong *et al* (1990) to study the role of sulphur, which I discuss below. Comparing the bonding of $[AlO_6]^{6-}$ and $[YO_6]^{6-}$ to a Ni_{10} cluster, Anderson *et al* found essentially no difference between them. This Ni_{10} cluster was then replaced by one containing (a) an Al atom, (b) an Y atom, (c) 10 Al atoms and (d) 10 Y atoms. The binding energy to Ni_{10}, Ni_9Y and Y_{10} increased in the sequence 4.0 eV, 5.8 eV and 12.8 eV. An increased binding due to Al was also calculated, although it was much less pronounced. The greatly increased binding due to Y was attributed to the mixing of its unoccupied d orbitals with the O 2p orbitals. It is consistent with the greater thermodynamic stability of Y–O bonds compared to Ni–O. Furthermore, the binding energy of Y to Ni was calculated to be much larger than that of Ni to Ni, due to charge transfer from Y 4d to the 3d band of Ni. While these calculations are suggestive, there are other candidate mechanisms for the RE effect which refer to the inhibition of interfacial diffusion by Y, or again to its effect as a sulphur trap in the bulk, which reduces the amount S which can segregate to and weaken the boundary.

Theoretical calculations of the effect of sulphur on metal–oxide adhesion are still very limited in number and scope, I am only aware of two which are based on electron theory. A first attempt was by Hong *et al* (1990), who studied some cluster models using a form of extended Hückel Hamiltonian. I summarize their work briefly here. They started by studying a Ni24 model (24-atom Ni cluster) of the Ni(110) surface, which had a six-atom surface layer, and a Ni25 model of a Ni(111) surface with a seven-atom surface layer. Predicted surface relaxations were in good agreement with experiment.

An unrelaxed Ni(111) model with 31 nickel atoms was used as a basis for studying bonding to S and to Al_2O_3. Adsorption of S was further modelled with a Ni(100) cluster of 16 atoms. The predicted S heights were in good agreement with experiment in each case.

The contact of Ni with an alumina basal plane was modelled with both oxygen-terminated (Al_4O_{18}), as described above, and aluminium-terminated (Al_9O_{24}) clusters. In the oxygen-terminated case, the cluster initially was given an excess charge of 15 electrons, simulating an O^- state of oxidation. For comparison, further electrons were added to convert this to O^{2-}. The strongest bonding, however, was between Al-terminated alumina and Ni, due to stabilization of the occupied Ni d orbitals by empty Al dangling bonds. It is speculated that such stable bonds might exist in reducing atmospheres.

The aluminium-terminated cluster was brought into contact with the Ni31 cluster on which three S atoms had been placed. Bonding was quite strong when the Al was above the S (2.46 eV per Al–S). When the clusters were oriented to bring Al above Ni, the bonding was weak, because the O–S closed-shell repulsion held the Al away from the Ni surface layer; the Al–Ni surface separation was 0.161 nm further than in the S-free interface. The O-terminated alumina clusters bonded only very weakly or not at all to the Ni surface with S present, again because of the O–S repulsion.

This is a non-self-consistent quantum mechanical approach. As we have seen, self-consistency is expected to be important for the energy of bonding in situations where an ion is bonding to a metallic surface. The limitations of the cluster approach are also apparent in the fact that the clusters have to be charged to prescribe the oxidation state of the oxygens at the interface. The authors emphasized strongly the sensitivity of the results to the unknown interfacial structures and compositions. The model of the weakening of the interfacial bonding by S which is tentatively suggested by these results is that the S, segregating at the interface, wedges apart the Al and Ni layers, which otherwise bond strongly. The S also repels O from the interface (closed-shell repulsion). In the absence of S, the weakest link at the interfaces is between the top two Ni layers. These authors did not address the question of how the adhesion would be modified if S were to enter substitutionally the first O layer of the alumina.

To my knowledge the only first-principles, self-consistent calculations of the effect of sulphur are those of Hong and co-workers (Hong *et al* 1995). These calculations are an extension of those by the same authors on Ag/MgO and Al/MgO described above. They considered two possible sites for the S atoms. In the first, referred to as interstitial, the S were located above the fourfold site at the metal surface, forming an extra plane (S_{int}) between metal and oxide. In the second, referred to as substitutional (S_{sub}), the S substituted for one of the surface oxygen atoms. In each case, and for both Al and Ag on MgO, the effect of S was to lower the ideal work of separation, as indicated in table 3.

Table 3. The ideal work of separation of metal/MgO interfaces (from Hong *et al* 1995)

Interface	MgO/Ag	MgO/S_{int}/Ag	MgO/S_{sub}/Ag	MgO/Al	MgO/S_{int}/Al	MgO/S_{sub}/Al
W_{sep} (J m^{-2})	1.9	0.74	1.5	1.1	0.68	1.0

The most dramatic effect of the interstitial S can be attributed to the S–O repulsion and the wider separation of the metal from the oxide in this case. In all cases, the metal–S bond is weaker than the metal–O bond, which can be understood on the basis of the larger ionic radius of S (0.190 nm) compared to O (0.146 nm). The inclusion of carbon in these interfaces had the opposite effect.

12. Summary and outlook

A qualitative picture of metal–ceramic bonding has emerged over the last twenty years, which is most well developed for wide-band-gap oxides. It was pioneered in the seventies and eighties by small electronic structure calculations, without taking into account the relaxation of ion positions. Minimization of the energy with respect to the ion positions first became possible in the nineties. Various approaches have developed in parallel. On the one hand simple tight-binding models gave qualitative insight into the nature of the states at the interface in an extended periodic system; on the other hand *ab initio* calculations, including geometry optimization, were applied to the simplest 10–20-atom periodic systems and revealed new details in electronic structure and bonding geometry. At an even simpler level of description, the image model of the adhesion was applied and shows some promise for modelling trends, and describing the effect of charged defects on adhesion. For this purpose the size of atoms is sometimes a useful concept. However, size is not everything as the above comparison of Ag with Al makes clear. It will also be interesting to see whether effects such as the difference between adhesion to AlN and Al_2O_3 can be so

simply explained. For this reason, it will be valuable to develop a database of high-quality *ab initio* calculations.

At this stage further work is necessary to establish the quantitative reliability of the *ab initio* methods for the work of separation of metal–ceramic interfaces. There is so far only one interface for which two independent *ab initio* calculations have been made, namely Ag/MgO. In this case there are two calculations for the monolayer of Ag and two for the multilayer. These are in very satisfactory agreement with each other regarding the absorption site and the bond lengths, but the works of separation do not agree so well. As shown in table 1, the Hartree–Fock (correlation-corrected) method and the LDA method for the monolayer differ by over 30%, or 270 mJ m^{-2}, and even the two LDA methods for the multilayer differ by about 15%, or 300 mJ m^{-2}. It should not be a major problem to investigate and reduce this level of uncertainty, just as much higher reliability has already been achieved in calculations of the binding energies of small molecules. The pseudopotential method is also likely to be increasingly applied to these systems. While it introduces an element of uncertainly besides the LDA, it is the first approach which has enabled a fully relaxed interface to be calculated, and more detailed calculations will reduce the uncertainties.

For correlated systems, such as the high-T_c cuprates, reliable methods of total energy and electronic structure calculation are being developed which will eventually also be applied to their interfaces with metals. Also magnetic films, of great interest to the manufacturers of recording equipment, may need theoretical approaches beyond LDA (spin polarized) or Hartree–Fock. The development and testing of such methods is still at an early stage, although electronic structure calculations for magnetic monolayers of Fe on Mg(001) have recently been made (Wu and Freeman 1994) using a spin-polarized density functional method. Because of the tools available to surface science, calculations relating to the early stages of growth of metal on ceramic, up to one or two monolayers, are most amenable to experimental testing.

Semi-empirical models of the tight-binding and image types will certainly be further refined and applied to more complicated simulations of interfacial phenomena, for which *ab initio* calculation will be too slow for many years to come. For example, it should be possible to study more quantitatively the role of misfit dislocations on the work of separation with simulation cells of a few thousand atoms—if the models are sufficiently reliable. To take another example, the processes of anion and cation diffusion at boundaries, as for example in oxide scale growth, are also a long way beyond the grasp of *ab initio* calculation and to study them quantitatively would require the development of a new approximate—but not too approximate—method of simulation. Another problem of interest in catalysis and in microelectronics is the controlled growth of thin films, and there is much to be learned about the nucleation and morphology of islands and the way they grow into layers. Works of adhesion, surfaces energies, point defect energies, diffusion barriers, ledge and corner energies and the energy of adsorption at various sites all play a part here. It will be valuable to calculate all these quantities for modelling purposes, since they are not always experimentally known or measurable. Whereas the calculations so far have been restricted to coherent interfaces, there is also a large experimental interest in the properties of interfaces with amorphous materials such as SiO_2. Approximations to such an interface will require cells containing a large number of atoms.

A degree of self-consistency, such as included in the LDA calculations referred to, is necessary for obtaining a reliable electronic structure, since it determines the alignment of the Fermi energy and possible band-bending effects. It is also a necessary ingredient for dealing with charged defects. Do charged defects in polyvalent oxides contribute significantly to

the adhesion, as the image model suggests, or is the basic reactivity of these metals such as Ti and Ni the dominant effect? This question will be resolved soon now that it is becoming feasible to treat somewhat larger numbers of atoms with *ab initio* simulation. The largest calculations could in a year or two be done on a teraflop computer. There are many theory groups now who could calculate say a twenty-atom system with their present 1 Gflop or so of available computer power. If we suppose a density functional method which for N atoms typically requires $O(N^3)$ computation time, these groups could calculate 200 atoms with a teraflop machine. This is a conservative estimate, since new algorithms are better than $O(N^3)$ and faster in other respects too. That puts many more complex interfaces within reach, and should make possible *ab initio* studies of segregation and its effect on structure and work of adhesion.

When segregation energies can be calculated, the way is open to calculating free energies and the chemical composition of interfaces as a function of, say, oxygen partial pressure. Free energies even for perfect interfaces have not yet been calculated on the basis of *ab initio* data, and this will be necessary step for any quantitative theory of high-temperature phenomena.

Experimental probes which can resolve the atomic structure and chemistry of metal–ceramic interfaces increase the challenge to make theoretical predictions of their electronic structure both for its own sake and as a route to predicting atomic structure. Besides calculating the ground-state geometry and electronic structure, theorists are now trying to calculate amplitudes and matrix elements for electronic transitions to excited states. This is necessary in order to interpret absorption spectroscopies such as EELS. The same theoretical techniques are required as for surface physics, but the calculations are more demanding computationally. The long-term goal of predicting electronic and mechanical properties of interfaces in specified chemical and thermodynamic conditions is a problem in materials science which bridges the traditional disciplines of solid-state physics and physical chemistry. Several models and calculations have been made, and although there has been some success, more questions have been raised than answers given. In view of the multitude of applications of the science of metal–ceramic interfaces, it is likely to remain a fertile area of collaborative research.

Acknowledgments

I have benefited from numerous discussions with colleagues, past and present, and visitors to the Max-Planck-Institut für Metallforschung in Stuttgart, who have shared their results with me, especially J Bruley, R Cannon, F Ernst, G Gutekunst, C Kruse, W Mader, J Mayer, G Möbus, M Rühle, U Schönberger and A Trampert. The work was supported in part by BRITE-EURAM under contract BRE2-CT94-0604. In part it resulted from a collaboration within, and was partially funded by, the Human Capital and Mobility Network on ‘Ab initio (from electronic structure) calculation of complex processes in materials’ (Contract ERBCHRXCT930369).

References

Alemany P 1994 *Surf. Sci.* **314** 114
Alemany P, Boorse R S, Burlitch J M and Hoffmann R 1993 *J. Phys. Chem.* **97** 8464
Anderson A B, Mehandru S P and Smialek J L 1985 *J. Electrochem. Soc.: Solid-State Sci. Technol.* **132** 1695
Bertrams T, Winkelmann F, Uttich T, Freund H J and Neddermeyer H 1995 *Surf. Sci.* **333** 1515

Bruley J, Brydson R, Müllejans H, Mayer J, Gutekunst G, Mader W, Knauss D and Rühle M 1994 *J. Mater. Res.* **9** 2574
Chan D K, Seidman D N and Merkle K L 1995 *Phys. Rev. Lett.* **75** 1118
Ching W Y and Xu Y-N 1994 *J. Am. Ceram. Soc.* **77** 404
Diebold U, Pan J-M and Madey T E 1995 *Surf. Sci.* **333** 845
Diebold U, Tao H-S, Shinn N D and Madey T E 1994 *Phys. Rev.* B **50** 14 474
Drevet B, Kalogeropoulou S and Eustathopoulos N 1993 *Acta Metall. Mater.* **41** 3119
Duffy D M, Harding J H and Stoneham A M 1993 *Phil. Mag.* A **67** 865
——1994 *J. Appl. Phys.* **76** 2791
——1995 *Acta Metall. Mater.* **43** 1559
Elssner G, Korn D and Rühle M 1994 *Scr. Metall. Mater.* **31** 1037
Ernst F, Pirouz P and Heuer A H 1991 *Phil. Mag.* A **63** 259
Espie L, Drevet B and Eustathopoulos N 1994 *Metall. Mater. Trans.* A **25** 599
Eustathopoulos N and Drevet B 1994 *J. Physique* III **4** 1865
Finnis M W 1991 *Surf. Sci.* **241** 61
——1992 *Acta Metall. Mater.* **40** S25
Finnis M W, Kaschner R, Kruse C, Furthmüller J and Scheffler M 1995 *J. Phys.: Condens. Matter.* **7** 2001
Finnis M W, Stoneham A M and Tasker P W 1990 *Metal-Ceramic Interfaces* ed M Rühle, A G Evans, M F Ashby and J P Hirth (Oxford: Pergamon) p 35
Freund H-J 1995 *Phys. Status Solidi* b **192** 407
Gota S, Gautier M, Douillard L, Thromat N, Duraud J P and Le Fèvre P 1995 *Surf. Sci.* **323** 163
Gubanov A I and Dunaevskii S M 1977 *Sov. Phys.–Solid State* **19** 795
Guénard P, Renaud G, Villette B, Yang M-H and Flynn C P 1994 *Scr. Metall. Mater.* **31** 1221
Gumbsch P, Daw M S, Foiles S M and Fischmeister H F 1991 *Phys. Rev.* B **43** 13 833
Gutekunst G, Mayer J and Rühle M 1994 *Scr. Metall. Mater.* **31** 1097
Heifets E, Orlando R, Dovesi R, Pisani C and Kotomin E A 1994 *Ab initio* simulation of the Ag/MgO interface *2nd Int. Conf. on Computer Simulation of Radiation Effects in Solids (Santa Barbara, 1994)* abstract
Heine V 1965 *Phys. Rev.* A **138** 1689
Henrich V E and Cox P A 1994 *The Surface Science of Metal Oxides* (Cambridge: Cambridge University Press)
Hoffmann R 1988 *Solids and Surfaces* (Cambridge: VCH)
Hong S Y, Anderson A B and Smialek J L 1990 *Surf. Sci.* **230** 175
Hong T, Smith J R and Srolovitz D J 1994 *J. Adhesion Sci. Technol.* **8** 837
——1995 *Acta Metall. Mater.* **43** 2721
Howe J M 1993 *Int. Mater. Rev.* **38** 233
Humenik J M and Kingery W D 1954 *J. Am. Ceram. Soc.* **37** 18
Ikuhara Y and Pirouz P 1993 *Ultramicroscopy* **52** 421
Jang H, Seidman D N and Merkle K L 1993 *Interface Sci.* **1** 61
Johnson K H and Pepper S V 1982 *J. Appl. Phys.* **53** 6634
Jones R O and Gunnarsson O 1989 *Rev. Mod. Phys.* **61** 689
Kasowski R V and Ohuchi F S 1988 *Phys. Rev.* B **35** 9311
Kasowski R V, Ohuchi F S and French R H 1988 *Physica* B **150** 44
Knauss D and Mader W 1991 *Ultramicroscopy* **37** 247
Kohn W and Sham L J 1965 *Phys. Rev.* A **140** 1133
Kohyama M, Ebata Y, Kose S, Kinoshita M and Yamamoto R 1990 *J. Physique Coll.* **51** C1 861
Kohyama M, Kose S, Kinoshita M and Yamamoto R 1992 *J. Phys. Chem. Solids* **53** 345
Kruse C 1994 *PhD Thesis* Stuttgart University
Kruse C, Finnis M W, Lin J S, Milman V Y, Payne M C, DeVita A and Gillan M J 1996 *Phil. Mag. Lett.* at press
Kruse C, Finnis M W, Milman V Y, Payne M C, DeVita A and Gillan M J 1994 *J. Am. Ceram. Soc.* **77** 431
Lambrecht W R L and Segall B 1992 *Acta Metall. Mater.* **40** S17
Li C, Fu R, Freeman A J and Fu C L 1993 *Phys. Rev.* B **48** 8317
Li J-G 1992 *J. Am. Ceram. Soc.* **75** 3118
Li S, Arsenault R J and Jena P 1988 *J. Appl. Phys.* **64** 6246
Libuda J, Bäumer M and Freund H-J 1994a *J. Vac. Sci. Technol.* A **12** 2259
Libuda J, Winkelmann F, Bäumer M, Freund H-J, Bertrams T, Neddermeyer H and Müller K 1994b *Surf. Sci.* **318** 61
Lundqvist S and March N H (ed) 1983 *Theory of the Inhomogeneous Electron Gas* (New York: Plenum)
Mader W 1989 *Z. Metall.* **80** 139
Mader W and Maier B 1990 *J. Physique Coll.* **51** C1 867

Mader W and Rühle M 1989 *Acta Metall.* **37** 853
Manassidis I, DeVita A and Gillan M J 1993 *Surf. Sci. Lett.* **285** L517
Mayer J, Flynn C P and Rühle M 1990 *Ultramicroscopy* **33** 51
Mayer J, Gutekunst G, Möbus G, Dura J, Flynn C P and Rühle M 1992 *Acta Metall. Mater.* **40** S217
Mehandru S P and Anderson A B 1991 *Surf. Sci.* **245** 333
Merkle K L 1991 *Ultramicroscopy* **130**
Merlin V and Eustathopoulos N 1995 *J. Mater. Sci.* **30** 3619
Möbus G 1995 private communication
Naidich J V 1981 *Prog. Surf. Membrane Sci.* **14** 353
Nath K and Anderson A B 1989 *Phys. Rev.* B **39** 1013
Nicholas M G and Mortimer D A 1985 *Mater. Sci. Technol.* **1** 657
Noguera C and Bordier G 1994 *J. Physique* III **4** 1851
Ohuchi F S and Kohyama M 1991 *J. Am. Ceram. Soc.* **74** 1163
Pan J M, Diebold U, Zhang L Z and Madey T E 1993 *Surf. Sci.* **295** 411
Peden C H F, Kidd K B and Shinn N D 1991 *J. Vac. Sci. Technol.* A **9** 1518
Pettifor D G and Cottrell A H (ed) 1992 *Electron Theory in Alloy Design* (London: The Institute of Materials)
Puska M J and Nieminen R M 1984 *Phys. Rev.* B **29** 5382
Rühle M, Evans A G, Ashby M F and Hirth J P (ed) 1990 *Metal–Ceramic Interfaces* (Oxford: Pergamon)
Rühle M, Heuer A H, Evans A G and Ashby M F (ed) 1992 *Proc. Int. Symp. on Metal–Ceramic Interfaces; Acta Metall. Mater.* **40**
Schönberger U, Andersen O K and Methfessel M 1992 *Acta Metall. Mater.* **40** S1
Shashkov D A and Seidman D N 1995a *Phys. Rev. Lett.* **75** 268
——1995b *Phys. Rev. Lett.* **75** 3588
Stobbs M 1995 private communication
Stoneham A M 1983 *Appl. Surf. Sci.* **14** 249
Tomsia A P, Saiz E, Dalgleish B J and Cannon R M 1995 *Proc. 4th Japan Int. SAMPE Symp. and Exposition (Tokyo)* Invited keynote lecture
Trampert A, Ernst F, Flynn C P, Fischmeister H F and Rühle M 1992 *Acta Metall. Mater.* **40** S227
Wu R Q and Freeman A J 1994 *J. Magn. Magn. Mater.* **137** 127
Yamamoto R, Kohyama M, Ebata Y and Kinoshita M 1989 *Proc. MRS Int. Mtg on Advanced Materials Ceramic Joints (Tokyo, 1988)* vol 8, p 183